Relaxation processes in one-dimensional self-gravitating many-body systems

Toshio Tsuchiya*
National Astronomical Observatory, Mitaka, 181, Japan

Naoteru Gouda
Department of Earth and Space Science, Osaka University, Toyonaka, 560, Japan

Tetsuro Konishi
Department of Physics, Nagoya University, Nagoya 464-01, Japan
(Received 26 May 1995)

Though one-dimensional self-gravitating N-body systems have been studied for three decades, the nature of relaxation is still unclear. There have been inconsistent results regarding the relaxation time; some initial states seemed to relax in the time scale $T \sim N\,t_c$, but other states did not relax even after $T \sim N^2\,t_c$, where t_c is the crossing time. The water-bag distribution was believed not to relax after $T \sim N^2\,t_c$. In a previous paper, however [Phys. Rev. E **50**, 2607 (1994)] we found that there are two different relaxation times in the water-bag distribution; in the faster relaxation (microscopic relaxation) the equipartition of energy distribution is attained but the macroscopic distribution turns into the isothermal distribution in the later relaxation (macroscopic relaxation). In this paper, we investigate the properties of the two relaxations. We find that the microscopic relaxation time is $T \sim N\,t_c$, and the macroscopic relaxation has the much longer time scale $4 \times 10^4 N\,t_c$, thus the water bag does relax. We can see that the inconsistency about the relaxation times is resolved as we see the two different aspects of relaxation. Further, the physical mechanisms of the relaxation are presented.

PACS number(s): 05.45.+b, 98.10.+z, 03.20.+i, 95.10.Ce

I. INTRODUCTION

One-dimensional self-gravitating many-body systems have been studied for three decades, both from astrophysical and chaotic dynamical interests. In the astrophysical point of view the system is a simple model of stellar systems, such as globular clusters, elliptical galaxies, and clusters of galaxies, and is convenient to draw out basic understanding of evolution and relaxation. On the other hand, it has been a problem in statistical mechanics whether all globally coupled systems with large degrees of freedom are ergodic and usual statistical mechanics is applicable.

Hohl [1–3] first asserted that there is a relaxation time scale of $N^2\,t_c$, where N is the number of particles and t_c is the characteristic time which is approximately the time for a member to traverse the system. In the late 1980s, however, several authors showed that there is no time scale of $N^2\,t_c$ in relaxation, but the character of evolution depends on the initial condition. A specific class of initial states (conterstreamed with virial ratio 0.3) appears to relax on the time scale $N\,t_c$ [4–6], which is much shorter than Hohl's prediction. On the other hand, other initial states with lower or higher virial rations take a much longer time to relax. In particular, the water-bag distributions do not appear to relax even after $N^2\,t_c$ [7,8]. Through these studies, one of the properties of evolution was recognized, which is that the systems do not relax directly to the thermal equilibrium, but to a quasiequilibrium after the violent evolution.

Severne and Luwel [9] suggested that there are three phases in relaxation. If the initial state is far from equilibrium, violent oscillation of the mean field gives rise to the violent relaxation [10] for the first several oscillations. This phase is called the *virialization phase*. After the system is almost virialized, remaining small fluctuations of the gravitational field cause the change of the individual particle energies. They called this era the *collisionless mixing phase*. After that, the *collisional relaxation phase* takes place, in which the particle interactions tend to drive the system towards the microscopic thermal equilibrium. This is the thermal evolution.

We have studied the evolution of the stationary water-bag initial distribution, which is believed not to relax to the thermal equilibrium. In this case, the virialization phase does not take place. In our previous paper [11] (we refer to it as Paper I), we showed that there exist two characteristic time scales even after the virialization phase. The shorter one is the *microscopic relaxation*, which means that mixing among energies of particles has developed completely as the result of mutual interaction but the global energy distributions are not transformed into that of the thermal equilibrium. This transformation occurs in a much longer time scale, which we refer to as the *macroscopic relaxation time*. The microscopic relaxation does not correspond to the collisionless mix-

*Electronic address: tsuchiya@yso.mtk.nao.ac.jp

ing because as compared with the microscopic relaxation, which leads the systems to the equipartition of energies, the collisionless mixing does not necessarily mean the equipartition.

Our aim is to understand the physical mechanism of the microscopic and macroscopic relaxations and then to resolve inconsistent results about the relaxation. Section II gives a description of our model and summarizes the evolution of the water-bag distribution found in Paper I. In Sec. III dependence of the microscopic relaxation on the number of the particles is studied numerically, and the physical interpretation is presented. In Sec. IV the macroscopic relaxation is considered, and conclusions and discussions are given in Sec. V.

II. MODEL

The system comprises N identical mass sheets, each of uniform mass density and infinite in extent in the (y, z) plane. We call the sheets *particles* in this paper. The particles are free to move along the x axis and accelerate as a result of their mutual gravitational attraction. The Hamiltonian of this system has the form

$$H = \frac{m}{2}\sum_{i=1}^{N} v_i^2 + (2\pi G m^2)\sum_{i<j}|x_j - x_i|, \tag{1}$$

where m, v_i, and x_i are the mass (surface density), velocity, and position of ith particle, respectively.

In our calculation, we employ the following scaling. The total mass $M = Nm = 1$, the total energy $E = 1/4$, and $4\pi G = 1$. With these normalizations, the units of length, velocity, and time are introduced as follows:

$$L = (4E)/(4\pi G M^2), \quad \text{unit of length}, \tag{2}$$

$$V = (4E/M)^{1/2}, \quad \text{unit of velocity}, \tag{3}$$

$$t_c = (1/4\pi G M)(4E/M)^{1/2}, \quad \text{unit of time}, \tag{4}$$

where t_c is referred to as *crossing time*, which is the typical time for a particle to traverse the system.

The potential of the system with finite N has no divergence, and the equienergy hypersurface is compact. Thus we can define the thermal equilibrium by the maximum entropy state. The distribution of particles in the thermal equilibrium is called the *isothermal distribution.* This equilibrium is the statistical equilibrium of the general kind for many-body systems. Figure 1 shows the isothermal distribution in μ space.

In addition to the thermal equilibrium, self-gravitating systems have another concept of equilibrium, *dynamical equilibrium.* It is defined mathematically in the continuous limit to an infinite number of particles in the system while the total mass is constrained to be finite. A state of the system is described by a distribution function $f(x, v)$, which is the number density of the particles at (x, v) in μ space. Since the mass of a particle goes to zero as the number of particles goes to infinity, the gravitational interaction between two constituents becomes negligible and the particles move by the force due to the mean potential Φ, where Φ is determined by the Poisson equation,

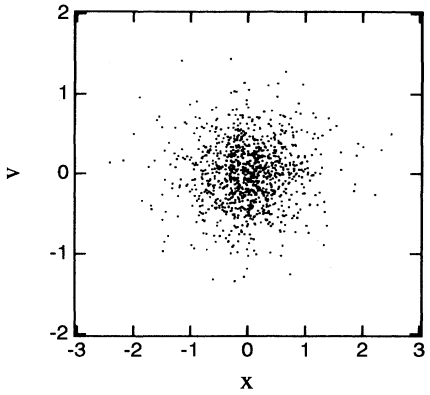

FIG. 1. The isothermal distribution in μ space. The number of particles is 1024. The full description of this distribution is given in Paper I.

$$\nabla^2\Phi = 4\pi G \int f(x, v)\, dv. \tag{5}$$

Dynamics of the system is subjected to the collisionless Boltzmann equation,

$$\frac{\partial f}{\partial t} + v\frac{\partial f}{\partial x} - \nabla\Phi(x)\frac{\partial f}{\partial v} = 0. \tag{6}$$

A dynamical equilibrium is a stationary solution of the Poisson and the collisionless Boltzmann equations. There exist many dynamical equilibria (see, e.g., [12]) including the *water-bag distribution*, which has a homogeneous phase density. We choose the water-bag distribution as one of our initial conditions. For the sake of simplicity, we distribute the particles uniformly in a rectangle region in the μ space with the virial ratio of unity (Fig. 2).

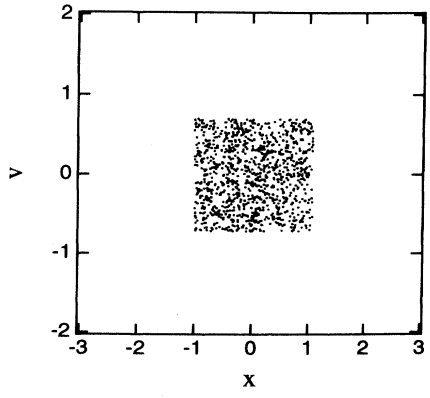

FIG. 2. The water-bag initial distribution in μ space. The number of particles is 1024. The full description of this distribution is given in Paper I.

It is not the exact stationary solution of the collisionless Boltzmann equation but it rapidly evolves to such an equilibrium very close to the stationary water-bag distribution.

The systems with the continuous medium approximate systems with finite but large number of particles. If the number is very large, a finite system stays in a dynamical equilibrium for a long time. However, it is not true equilibrium, and the scattering among the discrete particles transforms the state gradually from the dynamical equilibrium to the thermal equilibrium. We call this transition the macroscopic relaxation, in contrast with the microscopic relaxation, which leads the system to the equipartition of the individual energy. We summarize briefly the results of Paper I.

In Paper I, we introduced three quantities to analyze the evolution of the systems: the equipartition and the power spectrum density of fluctuation of individual particle energy, and the maximum Lyapunov exponent. The combination of these quantities revealed the microscopic evolution of the system. As a result, we can distinguish the two different time scales from the variation of the deviation $\Delta(t)$ from equipartition. The definition of $\Delta(t)$ is shown below.

The specific energy (energy per unit mass) $\varepsilon_i(t)$ of the ith particle is given by

$$\varepsilon_i(t) = \frac{1}{2}v_i^2(t) + 2\pi Gm\sum_{j=1}^{N}|x_j(t) - x_i(t)|. \tag{7}$$

If the evolution of the system is ergodic in the Γ space, the long time average of the specific energy takes a unique value for all i, i.e.,

$$\overline{\varepsilon_i} \equiv \lim_{T\to\infty}\frac{1}{T}\int_0^T \varepsilon_i(t)dt = \varepsilon_0 \equiv 5E/3. \tag{8}$$

The degree of deviation from equipartition is measured by the quantity

$$\Delta(t) \equiv \varepsilon_0^{-1}\sqrt{\frac{1}{N}\sum_{i=1}^{N}[\overline{\varepsilon_i}(t) - \varepsilon_0]^2}, \tag{9}$$

where $\overline{\varepsilon_i}(t)$ is the averaged value until t. In the numerical scheme, $\varepsilon_i(t)$'s are sampled at every crossing time t_c, and the average is defined simply by the summation of the samples divided by the number of the samples.

The variation of $\Delta(t)$ of the system with the water-bag initial distribution for $N = 64$ is shown in Fig. 3. The plateau at the beginning represents the collisionless phase, because in the collisionless phase the individual energies are conserved. After $t \sim 100$, $\Delta(t)$ begins to decrease as $t^{-1/2}$, which means that the fluctuation behaves in the same manner as thermal noise. The transition from const $\Delta(t)$ to the power law, $\Delta(t) \propto t^{-1/2}$, determines the microscopic relaxation. If the water-bag distribution is thermal equilibrium, then no more change is expected and $\Delta(t)$ goes to zero as t increases. However, it was found that $\Delta(t)$ increases at some $10^6\, t_c$. In Paper I, we studied what happens at the change. Not only $\Delta(t)$ but also the maximum Lyapunov exponent increased at that

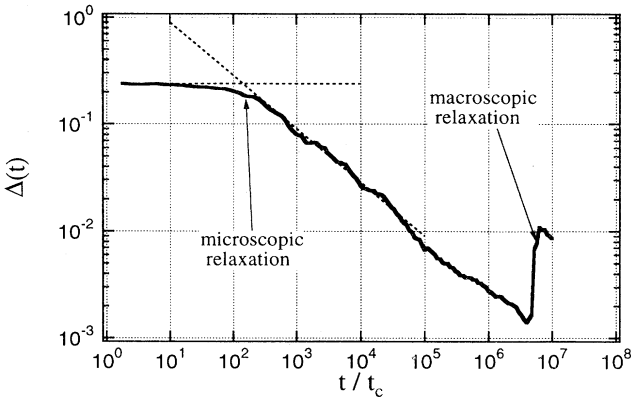

FIG. 3. The variation of the deviation from the equipartition $[\Delta(t)]$ for $N = 64$. Time is measured by the dynamical time. Two dashed lines are $\Delta(t)$, which is constant and proportional to $t^{-1/2}$. The bends of the $\Delta(t)$ correspond to the microscopic and the macroscopic relaxation time.

time and approached the value of the isothermal distribution. Further, the cumulative energy distributions and the power spectrum densities became that of the isothermal distribution. In this way, we concluded that the water bag is transformed into the isothermal distribution at that time. This increase of $\Delta(t)$ means that the dispersion of the energies averaged over the same time ($\sim 5 \times 10^6\, t_c$) is bigger in the isothermal distribution than in the water-bag distribution. The reason is that the isothermal distribution contains more high energetic particles so the amplitudes and the periods of the fluctuation are larger. In fact, we found that some particles stay at the highest energy for $10^5\, t_c$. From these facts, the macroscopic relaxation is estimated by the increase of $\Delta(t)$.

After the increase, $\Delta(t)$ begins to decrease again. Although we did not follow the evolution long enough after that, it seems that the decrease is proportional to $t^{-1/2}$. This is rather natural because the isothermal distribution is the true thermal equilibrium.

III. MICROSCOPIC RELAXATION

A. Numerical results

The microscopic relaxation means that the individual particle energies mix well so the system attains the equipartition. In Paper I we demonstrated that the diffusion of the individual energies are similar to random walk processes that yield the power spectrum density (PSD) of the Lorentz distribution, $P(f) \propto (f^2 + \gamma^2)^{-1}$, where γ is a constant. One way to determine the time scale of microscopic relaxation is to get the frequency $f \sim \gamma$, where the distribution changes its gradient. The reciprocal of γ gives the relaxation time scale. We chose another way to determine the time scale for the transition of variation of $\Delta(t)$ from a constant to $t^{-1/2}$. The relaxation time is sim-

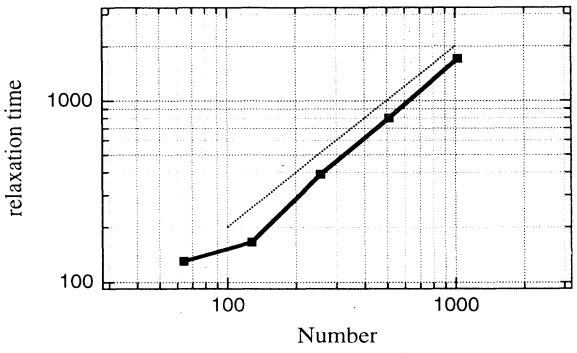

FIG. 4. The microscopic relaxation time for the systems with various number of the particles. The dotted line is $T = 2N$.

ply estimated by the crossing of two lines in Fig. 3: one is the constant $\Delta(t)$ and the other is $\Delta(t) \propto t^{-1/2}$. We examined 100 different initial states; all have the water-bag distribution macroscopically but are created from different random seeds at the initial time. The all 100 initial states are different only in the microscopic distribution. We found all runs gave almost the same microscopic relaxation time. Therefore, the time scale is universal for the water-bag distribution. Figure 4 shows the microscopic relaxation time for various N, the number of particles. We calculated $N = 64$, 128, 256, 512, and 1024. The dotted line in the figure is the line of $T = 2Nt_c$. The result tells us that the microscopic relaxation time T_m increases linearly as N increases;

$$T_m \sim N\, t_c. \tag{10}$$

Recently Reidl and Miller [13] found the same dependence of the time scale on which clustered initial states break into a quasiequilibrium. This correspondence is strong evidence that the microscopic relaxation is not special to the water-bag distribution, but rather general. Next we consider the physical mechanism of the relaxation.

B. Physical mechanism of the relaxation

The microscopic relaxation is the diffusion process that the energy of individual particles varies from the initial value. This variation causes the mixing of the energies and leads the system to equipartition. The Lorentz distribution of the PSD guarantees that the variation is the same as Brownian motion. The relaxation driven by Brownian motion in a stellar system is studied by Chandrasekhar [14–16] and several authors elaborated on the stochastic diffusion [17,18]. They suggest that the time scale becomes $\sim N\, t_c$, and our results confirm the idea. Here, it seems instructive to illuminate the simple picture of the mechanism.

Consider a particle located near the center at rest. The gravitational acceleration of the particle is proportional to the difference between the number of particles at the left side, $N_{\rm left}$, and the right side, $N_{\rm right}$, of the particle,

$$\dot{v} = 2\pi G m \left[N_{\rm right} - N_{\rm left}\right] . \tag{11}$$

The field particles travel across the system and the numbers of particles in both the left and the right sides fluctuate in time around their average. If we assume the fluctuation of the distribution of field particles is random and independent, the particle at the center has a random force,

$$\dot{v} \sim 2\pi G m \sqrt{N}. \tag{12}$$

Since this fluctuation is created by the motion of field particles, the typical lifetime of the fluctuation should be the crossing time,

$$t_c = \left[\frac{4\pi G N m}{L}\right]^{-1/2}, \tag{13}$$

where L is the length of the system.

The fluctuation of velocity, δv, caused by the random force is

$$\delta v \sim \sqrt{\pi G m L} \tag{14}$$

and if the fluctuations of field particle distribution occur independently, statistical theory asserts that the dispersion of the velocity fluctuation increases linearly in time,

$$(\delta v)^2 \frac{t}{t_c} . \tag{15}$$

Relaxation is accomplished when the dispersion grows as much as the typical value of velocity, V, in the system

$$V^2 \sim 4\pi G m N L. \tag{16}$$

Thus we get a time scale,

$$t \sim N\, t_c. \tag{17}$$

This time scale quite agrees with the numerical result [Eq. (10) and Fig. 4].

IV. MACROSCOPIC RELAXATION

Macroscopic relaxation occurs when the distribution is transformed from that of a dynamical equilibrium to that of the thermal equilibrium. The time scale of the transition from the water bag to the isothermal distribution is much larger than the microscopic relaxation time.

At the transition the distribution in the energy space becomes wider. The appearance of high energy particles causes an increase in the amplitude of the fluctuations. In order to examine this change, we introduce the locally averaged energy, which is defined by

$$\langle \varepsilon_i \rangle(t) \equiv \frac{1}{\Delta t} \int_{t-\Delta t}^{t} \varepsilon_i(t) dt. \tag{18}$$

We took $\Delta t \sim 20\,000$, which is much longer than the mi-

croscopic relaxation time in the water-bag distribution. By analogy with $\Delta(t)$, we introduce the deviation of the energy fluctuation from the equipartition value

$$\delta(t) \equiv \varepsilon_0^{-1} \sqrt{\frac{1}{N} \sum_{i=1}^{N} [\langle \varepsilon_i \rangle(t) - \varepsilon_0]^2}, \tag{19}$$

which gives the time variation of the energies averaged over Δt. The sudden increase of $\Delta(t)$ in Fig. 3 corresponds to the beginning of violent variation of $\delta(t)$ at $t \sim 5 \times 10^6 t_c$ in Fig. 5.

In the case of the microscopic relaxation of the water-bag distributions, different microscopic distributions (created by different random seeds) yield a definite relaxation time scale. For the macroscopic relaxation, however, we found a distribution of relaxation times that has a range over an order of magnitude. Therefore the mechanism of the macroscopic relaxation is surmised to be different from that of the microscopic relaxation. In this case, the distribution of the relaxation time is a big clue to finding the mechanism.

Figure 6 shows the probability distribution of the relaxation time of the system with $N = 64$. We took a statistical ensemble of 100 different initial states, as follows: As described in Paper I the initial states are realized by random distributions of particles which form uniform averaged phase density. Different seeds of the random number generator yield different random distributions microscopically but all gives the water-bag distribution macroscopically. The relaxation time of each run, T_M, is determined by the figure of $\delta(t)$, but there are wide variations within the ensemble. The relaxation times are divided into bins with the interval of $2 \times 10^6 t_c$. The solid diamonds represent the results of the numerical simulations. The vertical axis is scaled such that $P(T_M)\, dT_M$ gives the fraction of the number of runs, which fall into the interval dT_M. It is clear from the figure that the distribution has a exponential distribution,

$$P(T_M) = \frac{1}{\langle T_M \rangle} e^{-T_M/\langle T_M \rangle}, \tag{20}$$

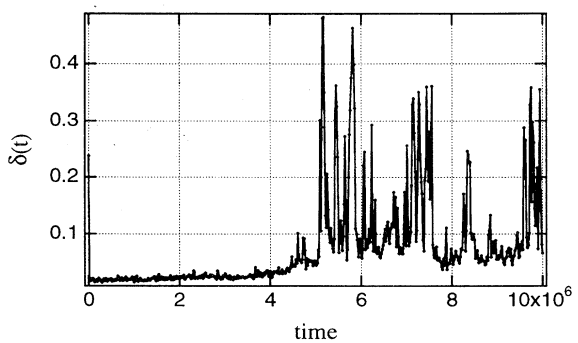

FIG. 5. The deviation of the locally averaged energies from the value of the equipartition. Individual energies are averaged over $20\,000 t_c$ around the given time t.

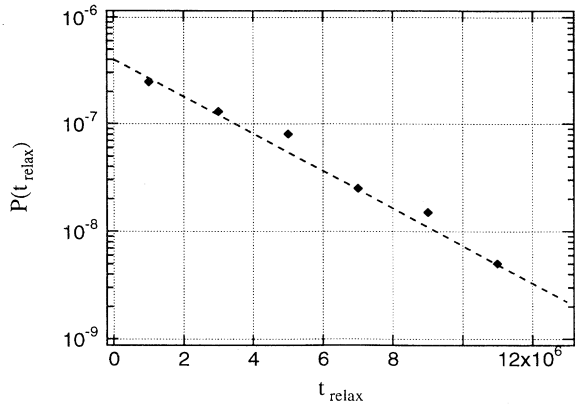

FIG. 6. The probability distribution of the macroscopic relaxation time of the system with $N = 64$. The relaxation times are calculated from the macroscopically same water-bag distribution but microscopically different random distribution realized by different seeds of random number generator.

where,

$$\langle T_M \rangle = 2.8 \times 10^6 t_c \qquad \text{for } N = 64, \tag{21}$$

and this gives the expectation value of the relaxation time.

Before we proceed to speculate on the mechanism it is useful to recall the phase space dynamics of the system: Any state of the system with N particles can be described by a certain point in the $2N$ dimensional phase space (Γ space). Each point yields some macroscopic distribution, such as the water bag or the isothermal. In Γ space, there is a region where all phase points yield the water-bag distribution. At the beginning the phase point is located in this region and then it moves out of the region as the system evolves. The macroscopic distribution is the water bag while the phase point stays in the region. When the point escapes from the region, the macroscopic distribution is transformed from the water-bag distribution into the isothermal because it is defined as the maximum entropy state, which means that it occupies the largest, and usually most of the region in the Γ space. Now we should explain the following facts.

(1) The water bag exhibits several properties of thermal equilibrium, such as convergence of Lyapunov exponents, and equipartition of energy, which suggest ergodicity.

(2) The probability distribution of the macroscopic relaxation time is an exponential function.

One possibility to explain these facts is that there exists a barrier which is an obstacle for a phase point to go out from the water-bag region. Due to this barrier a phase point is restricted in the region for a long time, where it travels all over the region as if the water-bag region is ergodic. However, the barrier is not perfect and there is a small gate from which a phase point in the water-bag region can escape. A phase point travels in the region in a very complicated way and is almost

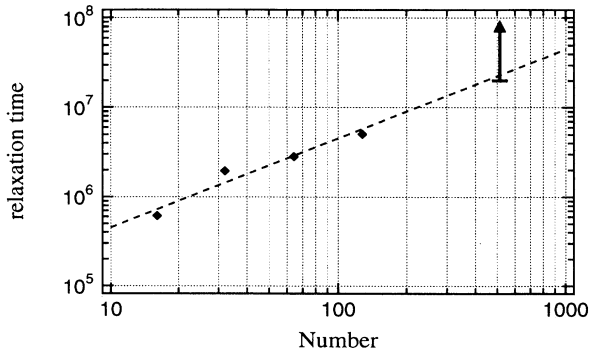

FIG. 7. The macroscopic relaxation time for the systems with various number of the particles. For $N = 512$, the ensemble of 50 water-bag distributions shows no relaxation until $T = 10^6 t_c$. The statistical analysis gives the true relaxation time which lies in the region restricted by the arrow in the 90% confidence level. The dashed line is $T = 4 \times 10^4 N$.

ergodic, thus the point finds the gate and escapes at random. Now we show a simple model which might well explain the numerical results as follows: as the simplest case, we assume that the escape probability is uniform in the region. Suppose that we have an ensemble of the phase points in the region. At the beginning the ensemble contains $n(0)$ points, but they escape from the region with constant rate $1/\langle T_M \rangle$, then the number of points which stay in the region at t decreases as $n(t)$. It is well known that $n(t)$ has the same form as Eq. (20). Therefore, this simplest model can explain the facts obtained by the simulations.

Next, in order to investigate the dependence of the time scale on the number of particles, the same procedure was applied to the system with different N; $N = 16$, 32, 128, and 512. Figure 7 shows the results. Especially for $N = 512$, we observed that 50 runs of the maximum integration until the time $T = 10^6 t_c$ did not relax. Thus we cannot determine the time of the relaxation for $N = 512$, but by assuming the exponential probability distribution, we can restrict the region where the *true* relaxation time probably lies. The arrow indicated the region of 90% confident level. These data are approximated by a linear relaxation

$$\langle T_M \rangle = 4 \times 10^4 N t_c, \tag{22}$$

which is shown by the dashed line.

V. CONCLUSIONS AND DISCUSSIONS

The numerical simulations of the one-dimensional self-gravitating many-body systems revealed the existence of two different kind of relaxations. One is the microscopic relaxation where the system attains the equipartition of individual energies though the macroscopic distribution shows no change. The other is the macroscopic relaxation where the macroscopic distribution is transformed into that of the thermal equilibrium.

We have shown the dependence of the microscopic and the macroscopic relaxation times on the number of the particles for the water-bag initial distributions. Our conclusions are summarized as follows.

(1) For the water-bag initial distributions, the microscopic relaxation time T_m is about N times the crossing time, $T_m \sim N t_c$.

(2) The physical mechanism of the microscopic relaxation is the diffusion of the energies of individual particles. Its driving force is the gravitational force of random fluctuation as a random force.

(3) The macroscopic relaxation time, where the transition of the macroscopic distribution from the water bag to the isothermal occurs, depends linearly on the number of the particles, $T_M \sim 4 \times 10^4 N t_c$.

(4) The macroscopic relaxation time T_M depends on initial conditions. It has exponential distribution as

$$P(T_M) = \frac{1}{\langle T_M \rangle} e^{-T_M/\langle T_M \rangle}. \tag{23}$$

(5) From the above facts, it is inferred that there is a region in Γ space where the macroscopic distribution yields the water bag, and a phase point is confined to the region for a long time, then it escapes through a small gate to the isothermal region at random. This hypothesis naturally explains why the water-bag behaves as if it is the thermal equilibrium, and why the macroscopic relaxation time has the exponential distribution.

The microscopic relaxation time $T_m \sim N t_c$ corresponds to the time scale found in Refs. [4,5,19], which concerned initial dynamical phase started from dynamically nonequilibria (the virial ratio is not unity). In such cases, both microscopic and macroscopic relaxations occur at the same time scale, thus the two relaxations were believed to be equivalent. The water-bag distribution had been known as one of the counterexamples of the relaxation of $N t_c$, because the water bag did not show the transformation of the macroscopic distribution to the isothermal distribution even after $N^2 t_c$ (for $N = 200$) [7,8]. We found, however, that the water-bag distribution does relax to the thermal equilibrium at the time scale much longer than the previous calculations. Luwel and Severne [8] already pointed out the existence of the collisionless mixing, which is equivalent to the microscopic relaxation in our papers. We determine the time scale as a function of the size of the system, which agrees that the relaxation time of the system evolved from dynamically nonequilibria.

In our hypothesis, the water-bag region is enclosed by some barrier, but what the barrier is, or how the motion of the phase point is restricted, is unknown. It could be that the water bag is the special case. However, if these properties are general for any stable dynamical equilibria, then the similar barriered regions are present outside the water-bag region. For instance, there is a fact that in the smaller systems ($N \leq 10$) the phase space is divided into segments [20]. Thus it is easy to surmise that the

barriered regions are the ruins of the segmentation.

The studies of individual orbits during the quasiequilibrium of the water bag and the transition to the isothermal will reveal the mechanism. We are working on the issue and will report it in the next paper.

ACKNOWLEDGMENT

The computation was carried out on Hewlett-Packard HP730 of the theoretical astrophysics division, National Astronomical Observatory.

[1] F. Hohl and D. T. Broaddus, Phys. Lett. A **25**, 713 (1967).
[2] F. Hohl and M. R. Feix, Astrophys. J. **147**, 1164 (1967).
[3] F. Hohl and J. W. Campbell, Astron. J. **73**, 611 (1968).
[4] M. Luwel, G. Severne, and P. J. Rousseeuw, Astrophys. Space Sci. **100**, 261 (1984).
[5] G. Severne, M. Luwel, and P. J. Rousseeuw, Astron. Astrophys. **138**, 365 (1984).
[6] C. J. Reidl, Jr. and B. N. Miller, Astrophys. J. **371**, 260 (1991).
[7] H. L. Wright, B. N. Miller, and W. E. Stein, Astrophys. Space Sci. **84**, 421 (1982).
[8] M. Luwel and G. Severne, Astron. Astrophys. **152**, 305 (1985).
[9] G. Severne and M. Luwel, Astrophys. Space Sci. **122**, 299 (1986).
[10] D. Lynden-Bell, Mon. Not. R. Astron. Soc. **136**, 101 (1967).
[11] T. Tsuchiya, T. Konishi, and N. Gouda, Phys. Rev. E **50**, 2607 (1994).
[12] J. Binney and S. Tremaine, *Galactic Dynamics* (Princeton Univ. Press, Princeton, 1987).
[13] C. J. Reidl, Jr. and B. N. Miller, Phys. Rev. E **51**, 884 (1995).
[14] S. Chandrasekhar, Astrophys. J. **93**, 285 (1941).
[15] R. E. Williamson and S. Chandrasekhar, Astrophys. J. **93**, 305 (1941).
[16] S. Chandrasekhar, Astrophys. J. **93**, 323 (1941).
[17] G. Severne and M. Luwel, Phys. Lett. A **104**, 127 (1984).
[18] B. N. Miller, J. Stat. Phys. **63**, 291 (1991).
[19] C. J. Reidl, Jr. and B. N. Miller, Phys. Rev. A **46**, 837 (1992).
[20] C. J. Reidl, Jr. and B. N. Miller, Phys. Rev. E **48**, 4250 (1993).